A Comparison of Property Estimators in Stereology and Digital Geometry

Yuman Huang and Reinhard Klette

CITR, University of Auckland, Tamaki Campus, Building 731
Auckland, New Zealand

Abstract. We consider selected geometric properties of 2D or 3D sets, given in form of binary digital pictures, and discuss their estimation. The properties examined are perimeter and area in 2D, and surface area and volume in 3D. We evaluate common estimators in stereology and digital geometry according to their multiprobe or multigrid convergence properties, and precision and efficiency of estimations.

Keyword: property estimation, stereology, digital geometry.

1 The Estimation Problem

A digital picture is a set of 2D or 3D digital data resultant from a process of digitization. Unlike sets in a continuous space, 2D or 3D data in digital pictures are presented in discrete form by a finite set of independent pixels or voxels. Perimeter and area in 2D, and surface area and volume in 3D are basic geometric properties which often need to be calculated. It is in general impossible to measure exact values (defined by sets in continuous space) of these properties if only a digital 2D or 3D picture is available. The precision of property estimators is important, and decisions need to be made about the type of estimator to be applied.

[10] reviews the history and methods in the field of picture-based property estimators. However, it does not discuss in detail how stereology methods relate to methods popular in digital geometry. Gauss (1777-1855) studied the estimation of area by counting grid points, and this method is actually applied in stereology as well as in digital geometry. Thompson (1930) and Glagolev (1993) are cited in [14] for the origins of the point count method in quantitative microscopic analysis which is a predecessor of stereology.

Both stereology as well as digital geometry are mainly oriented towards property estimations. Stereologists estimate geometric properties based on stochastic geometry and probability theory [13]. Key intentions are to ensure isotropic, uniform and random (IUR) object-probe interactions to ensure the unbias of estimations. The statistical behavior of property estimators is also a subject in digital geometry. But it seems that issues of algorithmic efficiency and multigrid convergence became more dominant in digital geometry.

Both disciplines attempt to solve the same problem, and sometimes they follow the same principles, and in other cases they apply totally different methods. In this paper, a few property estimators of stereology and digital geometry are comparatively evaluated, especially according to their multiprobe or multigrid convergence behavior, precision and efficiency of estimations.

2 Stereology and Digital Geometry

Digital geometry is the study of geometric properties of subsets of digital pictures. It includes ways of digitizing objects and also the estimation of their geometric properties based on the results of digitization (discrete data instead of continuous Euclidean data).

Stereology is a way of estimating geometric properties of objects in a multidimensional space by observing its lower dimensional structures [15]. It is used broadly in some fields such as material science, biology and biomedicine for examining the microstructure of objects such as materials [14], biological tissues [13], and human organs.

There are a number of commercial groups targeting computerized stereology to solve real-world problems, such as MicroBrightField Inc., Olympus Denmark (recently merged with Visiopharm), Kinetic Imaging Ltd., SPA Inc., R & M Biometrics Inc. These companies have made computer-based stereology systems (Stereo Investigator, CAST, Digital Stereology, Stereologer, Stereology Toolkit) either as a complete package, including advanced hardware (like a light microscope), accompanying software, or software toolkits for supporting stereological analysis.

Since these systems are also computer-based, digital techniques must be used. The data which they process are digitized and discontinuous. The digitization model used in stereology may vary, but it is always within the scope of digital geometry. To the best of the author's knowledge, no wide-scale comparison has ever been made so far in public for comparing accuracy or efficiency of stereology or digital geometry methods.

From the theoretical point of view, one opportunity for comparison is to study how testing probe and resolution affect the accuracy of estimations. We define multiprobe convergence in stereology analogously to multigrid convergence in digital geometry. Both definitions can be generalized to cover not only the estimation of a single property such as length, but also of arbitrary geometric properties, including area in 2D, and surface area and volume in 3D.

2.1 Stereology

Measurements follow stereological formulas, which connect the measurements obtained using different probes with the sought properties.Table 1 contains basic stereological formulas using standard notion of stereology (see, e.g., [7, 13, 15, 17] and further below for definitions of these notations).

We define multiprobe convergence in stereology analogously to multigrid convergence in digital geometry.

Property	Basic formulas	Derived formulas
Perimeter	$P_L = \frac{2}{\pi} \cdot L_A$; $P_L = \frac{P}{L_T}$	$L_A = \frac{\pi}{2} \cdot P_L$; $\widehat{L} = L_A \cdot L_T$
Area	$A_A = P_P$	$\widehat{A} = A_A \cdot P$
Surface area	$S_V = 2 \cdot \frac{P_L}{L_T}$	$\widehat{S} = S_V \cdot V_T$
Volume	$V_V = P_P$	$\widehat{V} = V_V \cdot V_T$

Table 1. Basic stereological formulas.

Definition 1. *Let Q be the object of interest for estimation, and assume we have a way of obtaining discrete testing probes about Q. Consider an estimation method E which takes testing probes as input and estimates a geometric property $X(Q)$ of Q. Let $X_E(T_n)$ be the value estimated by E with input T_n, where T_n contains exactly $n > 0$ testing probes. The method E is said to be* multiprobe convergent *iff it converges as the number n of testing probes tends to infinity (i.e., $\lim_{n\to\infty} X_E(T_n) = c,\ c \in \mathbb{R}^2$), and it converges to the true value (i.e., $c = X(Q)$).*

Testing probes are measured at, along or within points, lines, planes, disectors and so forth. The geometric property $X(Q)$ might be the length (e.g., perimeter), area, surface area, or volume, and we write L, A, S, or V for these, respectively. (Note that the true value $X(Q)$ is typically unknown in applications.) The method E can be defined by one of the stereological formulas.

2.2 Digital Geometry

The grid resolution h of a digital picture is an integer specifying the number of grid points per unit. There are different models of digitizing sets Q for analyzing them based on digital pictures. Grid squares in 2D or grid cubes in 3D have grid points as their centers. The Gauss digitization $G(Q)$ is the union of the grid squares (or grid cubes) whose center points are in Q. The study of multigrid convergence is a common approach in digital geometry [10]. However, we recall the definition:

Definition 2. *Let Q be the object of interest for estimation, and assume we have a way of digitizing Q into a 2D or 3D picture P_h using grid resolution h. Consider an estimation method E which takes digital pictures as input and estimates a geometric property $X(Q)$ of Q. Let $X_E(P_h)$ be the value estimated by E with input P_h. The method E is said to be* multigrid convergent *iff it converges as the number h of grid resolution tends to infinity (i.e., $\lim_{n\to\infty} X_E(P_h) = c,\ c \in \mathbb{R}^2$), and it converges to the true value (i.e., $c = X(Q)$).*

For simplicity we assume that our 2D digital pictures P_h are of size $h \times h$, digitizing always the same unit square of the real plane. Analogously, we have $h \times h \times h$ in the 3D case.) An estimation method in digital geometry is typically defined by calculating approximative geometric elements (e.g. straight segments,

surface patches, surface normals) which can be used for subsequent property calculations.

3 Estimators

The estimators of our experimental evaluation fall the stereology or digital geometry category, and they may have varying definitions within their category, for example, by the different use of probes or by different bases.

Perimeter and surface area estimators in stereology and in digital geometry are totally different by applied method. In stereology, for example a line testing probe (a set of parallel straight lines in 2D or 3D space) is used, and the perimeter or surface area of an object is approximated by applying stereological formulas with the count of object-line intersections. A testing probe for a surface area estimator may be formed by a set of cycloids, and must be used with vertical uniform random (VUR) segments [1].

In digital geometry, estimators for measuring perimeter or surface area can be classified as being either local or global (see, e.g., [4, 9, 10]). [16] suggested using a fuzzy approach for perimeter and area estimations in gray level pictures. The chosen perimeter estimator for our evaluation (for binary pictures) is global and based on border approximations by subsequent digital straight segments (DSS) of maximum length.

The surface area can be estimated for "reasonable small" 3D objects by using time-efficient local polyhedrizations such as weighted local configurations [12]. For higher picture resolutions it is recommended to apply multigrid convergent techniques. For example, [10] illustrates that local polyhedrizations such as based on marching cubes are not multigrid convergent. Global polyhedrization techniques (e.g., using digital planar segments) or surface-normal based methods can be applied to ensure multigrid convergence. Because of the space constraint, none of these surface area estimators are covered in this paper. The 2D area and volume estimators of stereology and those of digital geometry follow the same point-count principle. In stereology, a point probe (a set of systematic or random points) is placed in 2D or 3D space, the points within the object are counted, and the stereology formulas are applied to estimate the area or volume of an object of interest. (The proportion of points within an object reflects the area or volume density of the object.)

The Cavalieri principle was defined for volume estimations in stereology. Following this, a point probe is used on a set of parallel planes intersecting the 3D object. The product of the sum of the estimated area of object segments and the distances between planes approximates the volume of a 3D object. Both volume estimators (using a 3D point probe or a 2D plane probe with a point probe on every plane) are merging into one methods when the distance between planes is equal to a regular interspacing between points in 2D which are placed on these planar sections.

In digital geometry, a common estimator of area is pixel counting, whereas that of volume is voxel counting. These two estimators are also a special case

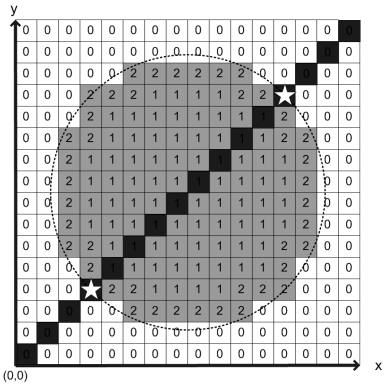

Fig. 1. 8-border pixels are labeled by 2, and 8-inner pixels by 1.

of point counting in stereology where a set of pixel or voxel centers is used as the point probe. Because the resolution directly relates to the number of pixels or voxels in the digital picture, it will consequently affect the precision of estimations if the stereological formulas are applied.

The performance of estimators is discussed under the condition that cost of digitization is excluded.

3.1 Perimeter and Surface Area

Line intersection count method (LICM) is a common stereology estimator for 2D perimeter and 3D surface area. This estimator involves four steps: generate a line probe, find object border in a digital picture, count object-probe intersections, and apply stereological formulas to obtain an estimation of the property.

The line probes in 2D or 3D may be a set of straight or circular lines (see, e.g., [7, 13, 15]), or made up of cycloid arcs [1]. Since a set of straight lines can be easily represented by general straight line functions, we use them as the testing probe of both perimeter and surface area estimations.

There are many possible ways of defining a digital line (see, e.g., [10]). In this paper, a 2D or 3D straight line in digital pictures is represented as a sequence of pixels or voxels whose coordinates are the closest integer values to the real ones. The integer coordinates of line pixels can be calculated using the midpoint line scan-conversion algorithm in [6], which is based on the Bresenham algorithm [2]. The length of a 2D [3D] digital line segment is the Euclidean distance between its start point (x_0, y_0) $[(x_0, y_0, z_0)]$ and end point (x_1, y_1) $[(x_1, y_1, z_1)]$. There exist different options for defining borders of objects in 2D or 3D pictures. In this paper, in 2D the 8-border of Q is used to observe intersections between Q and the line probe, whereas in 3D the 26-border of Q is used (for definitions of 8-border or 26-border see, for example, [10]). Isotropic, uniform, and random (IUR) object-probe intersections are required for obtaining unbiased estimation results. Digital lines are ordered by scanning direction. Figure 1 shows a 45°

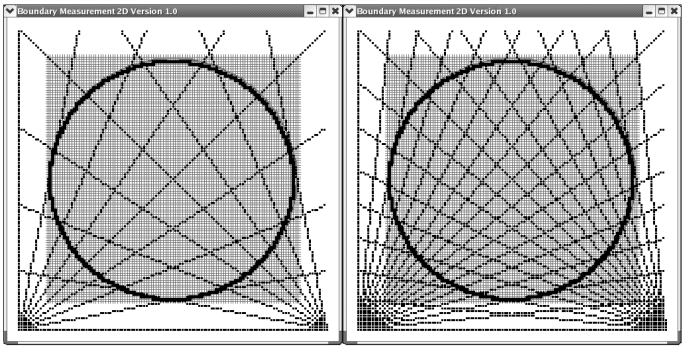

Fig. 2. Screen shots of pivot lines of the LICM estimator using line probes of 16 (left) and 32 (right) directions.

digital line intersecting the 8-border of Q in a 16×16 picture. Note that any digital line (which is an 8-curve) intersects an 8-border (which is a 4-curve) if it "passes through".

Definition 3. *A pixel (voxel) visited along a digital line is an* intersection *iff it is an 8-border pixel (26-border voxel) of the object Q and successor (along the line) is a non-border pixel (voxel).*

Since the objects of interest are general (not specified as a certain type), they may not be IUR in 2D or 3D space. To ensure IUR object-probe intersections, either the object or the probe must be IUR, or the combination of both must be isotropic [13]. In the experiments we attempt to generate an IUR straight line probe for the stereology estimator (LICM) to produce unbiased results for perimeter and surface area measurements.

Perimeter The perimeter estimators examined are the stereology estimator (LICM) and the digital geometry estimator based on maximum length digital straight segments (DSS).

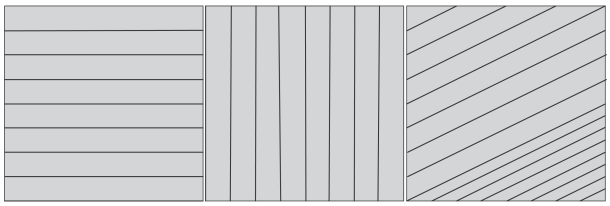

Fig. 3. Assume $h = 8$ (i.e., an 8×8 picture). Left: in horizontal direction we have a total of h lines. Middle: in vertical direction, we also have a total of $h$lines. Right: in any other direction (i.e. not equal to 0° or 90°) we have a total of $2h - 1$ lines.

The stereology estimator corresponds to the stereological formula

$$L_A = \frac{\pi}{2} \cdot P_L = \frac{\pi}{2} \cdot \frac{P}{L_T}$$

which is basically the calculation of perimeter density (length per unit area) of a 2D object. P is the number of intersections between line probe and (border of the) object Q. L_T is the total length of the testing line probe, and P_L is the point count density (intersections per unit length). As a corollary of this, the perimeter of an object can be estimated by multiplying L_A by the total area A_T that the line probe occupies:

$$\widehat{L} = L_A \cdot A_L = \frac{\pi}{2} \cdot \frac{P}{L_T} \cdot A_T$$

At the beginning of our experiments we consider how the estimation precision is influenced by an increase in the number of directions n of line probes. The direction of line probes are selected by dividing 180° equally by n. For instance, if there are 4 directions required, then lines of slopes 0°, 45°, 90°, and 135° are generated. Figure 2 illustrates the lines for 16 or 32 directions. Note that only one "pivot line" per direction is shown in this figure.

To avoid errors or a bias caused by direction or position of line probes, every pivot line of one direction is shifted along the x and y axes by just one pixel; see Figure 3. Assume that the pivot line which is incident with $(0, 0)$ (i.e., the left lower corner of a picture) intersects the frontier of the unit square $[0, 1] \times [0, 1]$ again at point p, with an Euclidean distance L between $(0, 0)$ and p. The total length of a line probe in direction 0°, 45° or 90° is hL, and equal to

$$\frac{3h - h \tan \alpha}{2} L$$

where α is the smaller angle between 0° and 45° defined by the pivot line in our unit square.

However, a stereological bias [13] can not be avoided in this case due to the preselection of start position and direction of line probes for perimeter estimation of non-IUR objects. Therefore, we also include an estimator which uses lines at random directions, generated using a system function *rand()* (which is supposed to generate uniformly distributed numbers in a given interval). Although a random number generator is used, the generated line probes are not necessarily isotropic in 2D space. (An improved IUR direction generator is left for future research.) For the digital geometry estimator DSS, we start at the clockwise lower-leftmost object pixel and segment a path of pixels into subsequent DSSs of maximum length. Debled-Rennesson and Reveillès suggested an algorithm in [5] for 8-curves, and earlier Kovalevsky suggested one in [11] for 4-curves. In our evaluation, both methods have been used, but we only report on the use of the second algorithm (as implemented for the experiments reported in [8]) in this paper.

The DSS estimator is multigrid convergent, whereas the multiprobe convergent behavior of the LICM estimator depends on the used line probe. If the

line probe is a family of sets of parallel straight lines at equal distances, each set for a different direction, then the LICM estimator appears to be multiprobe convergent.

The digital geometry estimator DSS is time-efficient because it traces only borders of objects, and used one of the linear on-line DSS algorithms.

The time-efficiency of the stereology estimator LICM depends on the number of line pixels involved, since it checks every pixel in a line probe to see whether there is an intersection. In both implementations of LICM (i.e., n directions by equally dividing 180°, and random directions generated by the system function *rand()*), every pivot line into one direction is translated along x- and y-axes at pixel distance (as shown in Figure 3), which results into multiple tests (intersection?) at all pixels just by considering them along different lines. In case of pictures of "simple objects" we can improve the efficiency by checking along borders only instead of along all lines. However, normally we can not assume that for pictures in applications.

Surface Area We tested speed and multiprobe convergence of the stereology estimator LICM for surface area measurements, using the stereological formula

$$S_V = 2 \cdot I_L = 2 \cdot \frac{P_L}{L_T}$$

where I_L is the density of intersections of objects with the line probe, and this is equal to the result of the line intersection count P_L divided by the total length L_T of the line probe.

Consequently, the surface area of Q can be estimated by multiplying its surface density (obtained from the previous relationship) by the total volume of the testing space V_T (i.e., h^3, which is the occupied volume of a 3D picture), $\widehat{S} = S_V \cdot V_T$.

Similar to the stereology estimator of perimeter measurement, a way of creating an IUR straight line probe in 3D is required for unbiased surface area estimations. The LICM estimator may not be multiprobe convergent because of the used line probes. The efficiency of the estimator depends on the total number of line voxels.

3.2 Area and Volume

The stereology estimator for both 2D area (3D volume) measurements counts 2D (3D) points which are within the object of interest. When the point probes used are the centers of *all* pixels (voxels) of a given picture, then this estimator coincides with the method used in digital geometry.

Basic stereological formulas (see, e.g., [7]) such as

$$\widehat{A} = A_P \cdot P = \frac{A_T}{P_T} \cdot P = \Delta x \cdot \Delta y \cdot P$$

are applied for 2D area estimation. The area of an object A can be estimated by multiplying the number of incident points P by the area A_P per point. In other words, the area occupied by all incident points approximates the area of the measured object. The area A_P per point is the total area A_T of the picture (i.e., width Δx times height Δy) divided by the total number P_T of points of probe T.

The principle of Bonaventura Cavalieri (1598-1647), see [3], is suggested for estimating the volume of an object Q in 3D space in stereology books such as [7, 13, 15]. [13] combines the Cavalieri principle with the point count method. A series of parallel 2D planes is used as test probe, where a set of points is placed into each plane to obtain the intersected area of the plane with the object. If there are m planes used in the process, the volume of the object V can be estimated by multiplying the distance θ between the planes by the sum of the intersected areas $A_1, A_2, A_3, \ldots, A_m$ of all planes, $\widehat{V} = \theta \cdot (A_1 + A_2 + A_3 + \cdots\ A_m)$.

Russ and Dehoff use a set of 3D points as the test probe in [15] to estimate the volume fraction V_V from calculating a point fraction P_P, the ratio of incident points P (with the object) to the population of points P_T, $V_V = P_P = \frac{P}{P_T}$. As a corollary of this, the volume V of the object is equal to the product of the volume fraction and the total volume occupied by the testing probe V_T (i.e., h^3 in an $h \times h \times h$ picture), which can be calculated by multiplying the number of incident points by the volume per point V_P,

$$\widehat{V} = V_V \cdot V_T = \frac{P}{P_T} \cdot h^3 = P \cdot V_P$$

The results of both methods are identical when all the 2D planes are coplanar at equal distances, the set of points chosen in every plane is uniform, and the interspacing between these 2D points equals to the distance between planes.

For area and volume estimations, since the estimators in both fields follow the same point count principles, the choice of point probes will definitely influence the performance of the algorithm. If a point probe is randomly picked from regular 2D or 3D grid points, and the chosen number of points is less than the total number of pixels or voxels in the picture, then the method is (trivially) more time-efficient than the digital geometry approach.

Area and volume estimators are "very precise", suggesting a fast multiprobe convergence (see experiments in Section 4); they have been widely used in research and commercial fields. The digital geometry estimators (i.e., considering all pixels or voxels) are known [10] to be multigrid convergent (e.g., for particular types of convex sets).

4 Evaluation

We tested 2D perimeter and area estimators by using six objects shown in Figure 4. For the area of the lunula we used the formula $b \cdot r - a(r - h)$ for the area of the "removed" segment of the disk, with arc length $b = 2\pi r \cdot \alpha/360$ (using integral part $\alpha = 139$ of the estimate $\alpha = 139.0253698\ldots$), segment height $h = 0.26$, and $a = 2 \cdot \sqrt{0.1404}$.

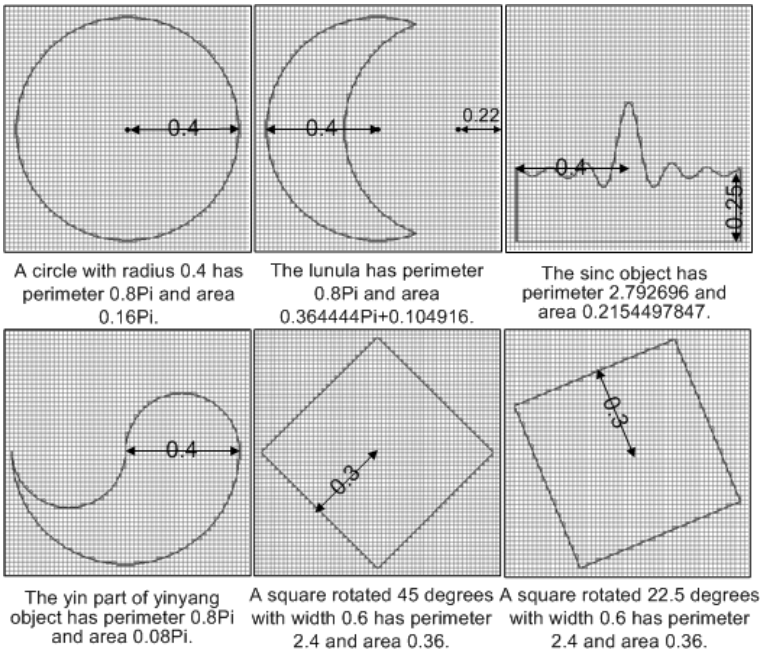

Fig. 4. Six pictures suggested as test data in [8].

In case of 3D objects, we used a cylinder, sphere, cube, and an ellipsoid for volume estimation, and the first three objects are also used for surface area estimation.

The relative error E_r of experiments is a percentage, it is equal to the absolute value of the estimated value V_e minus the true value V_t, divided by the true value, then multiplied by 100, $E_r = \frac{|V_e - V_t|}{V_t} \cdot 100$.

4.1 Perimeter and Surface Area

We compare results of the DSS estimator, the LICM estimator with four preselected directions (which are 0°, 45°, 90°, and 135°), and the LICM estimator with four random directions (called LICM_R; generated using the system function *rand()*), see Figure 5.

The obtained results show that the precision of the DSS estimator is the best of these three estimators, whereas the precision of the LICM estimator with four preselected directions is better than that of LICM_R. Multiprobe or multigrid convergence is apparent in most of the diagrams. Obviously, four random numbers are not "able" to define an IUR direction generator. (The figure shows results for directions 151.23°, 70.99°, 140.96° and 143.72°; LICM_R appears to be not multiprobe convergent on the circle, lunula, and square rotated 22.5° for these values.) Figure 6 illustrates the relative errors averaged over all six test

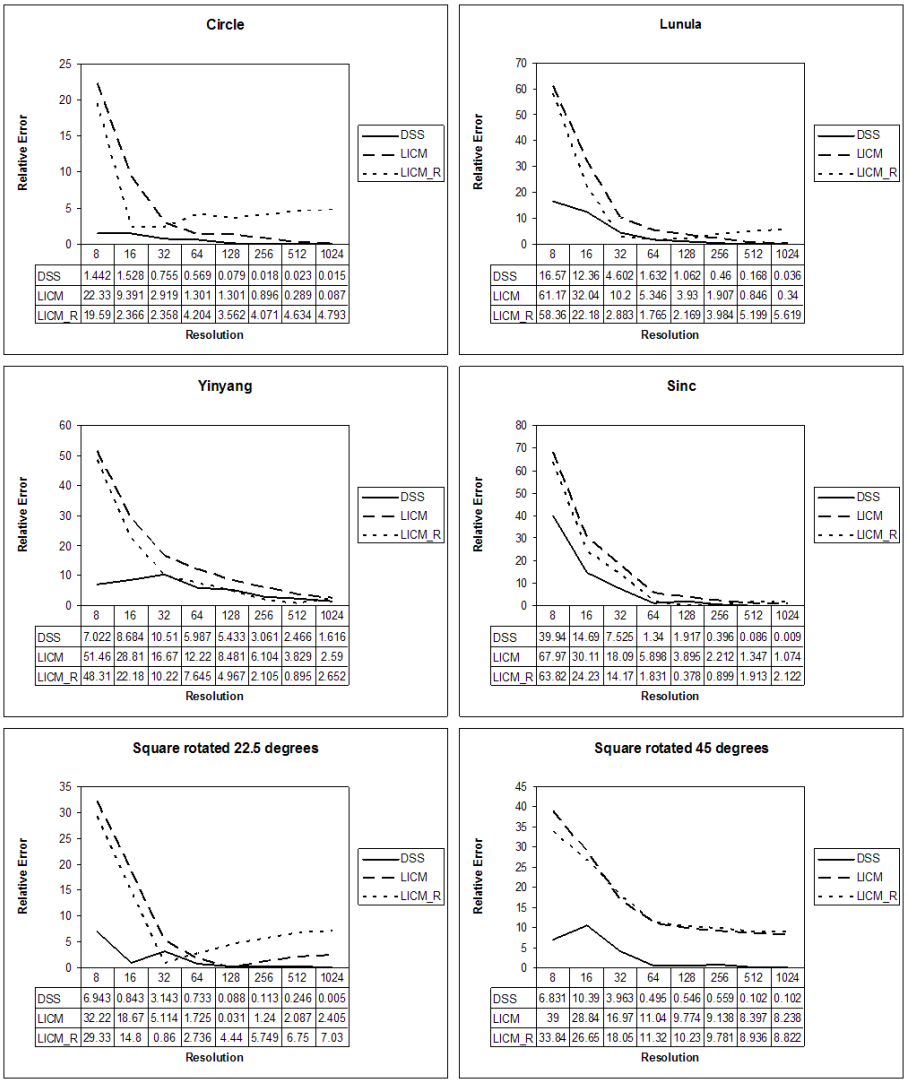

Fig. 5. Comparison of DSS, LICM (4 directions) and LICM_R (LICM with 4 random directions) on six test objects.

objects. The obtained LICM_R errors are slightly increasing between resolution 256 and 1024.

We also tested the multiprobe behavior for an increase in numbers of directions (up to 128 different directions in experiments). Surprisingly, results did not steadily improve by increasing the number of directions for LICM or LICM_R, and in some cases the error even increased for larger numbers of directions. See

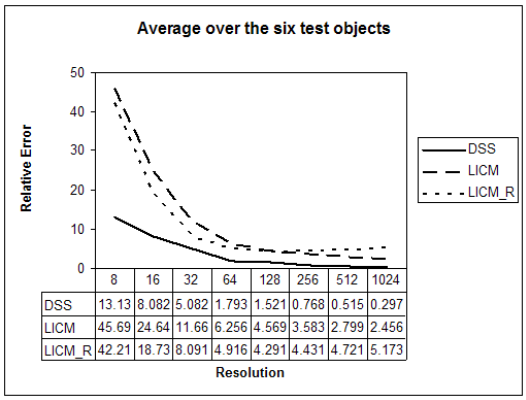

	8	16	32	64	128	256	512	1024
DSS	13.13	8.082	5.082	1.793	1.521	0.768	0.515	0.297
LICM	45.69	24.64	11.66	6.256	4.569	3.583	2.799	2.456
LICM_R	42.21	18.73	8.091	4.916	4.291	4.431	4.721	5.173

Fig. 6. Comparison of average relative errors over all the six test objects, for DSS, LICM and LICM_R.

Figure 7 for the example of a disk, where the error is smallest in general for just 4 directions! A possible explanation is that more directions increase the number of lines which do not intersect the circle at all.

The surface area of 3D objects is estimated using the LICM_R estimator with digital rays in 3D space starting at random positions, and into random directions (generated by the system function *rand()*. (We tested up to a picture resolution of 128. Rays are only traced within the space of the picture.) Now, in 3D space we generated every ray individually (i.e., not shifting pivot lines or rays anymore as in 2D). So, the number of rays is now reduced to be equal to the number of directions!

Figure 8 shows results for a constant resolution ($h = 128$) and increases in numbers of directions (i.e., numbers of rays). Figure 9 shows results for a

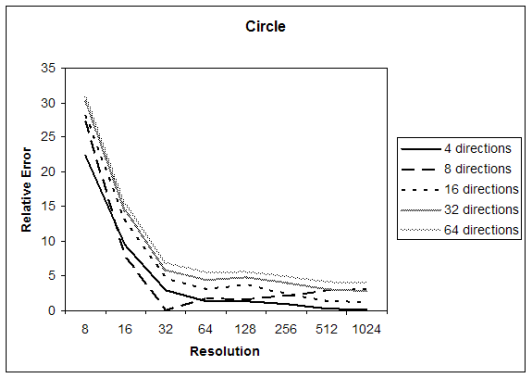

Fig. 7. LICM-estimation of the perimeter for the disk using different numbers of directions.

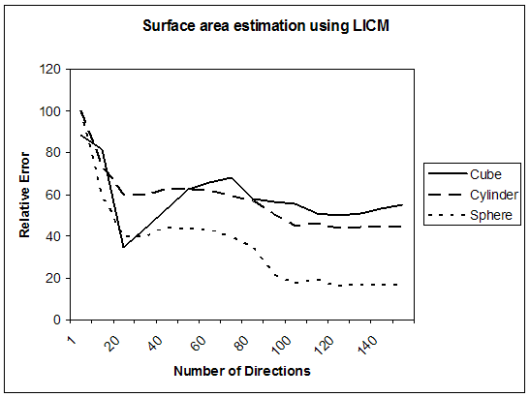

Fig. 8. LICM_R-estimation of surface area for the cube, cylinder, and sphere using a 128×128 picture.

constant number of directions (100), and an increase in picture resolution. The results indicate relatively large errors. (Obviously, this is certainly related to the smaller number of rays compared to the number of lines in 2D.) However, it can be seen that the results for the sphere are better than those for the cube and cylinder in both Figures.

4.2 Area and Volume

The results shown in Figure 10 are using the pixel count estimator which checks all 2D grid points of the picture. They are very precise on all six test objects, always with less than 0.1 percent error from the true area when the picture resolution is 1024.

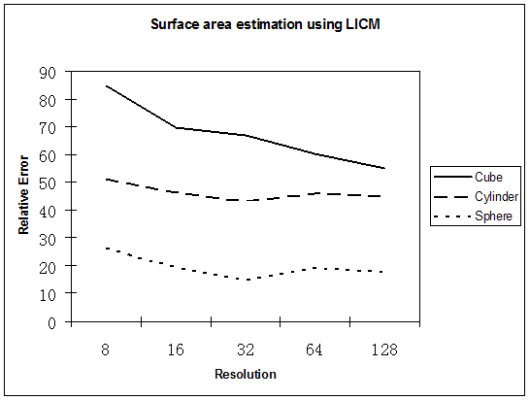

Fig. 9. LICM_R-estimation of surface area for the cube, cylinder, and sphere using 100 lines at different picture resolutions.

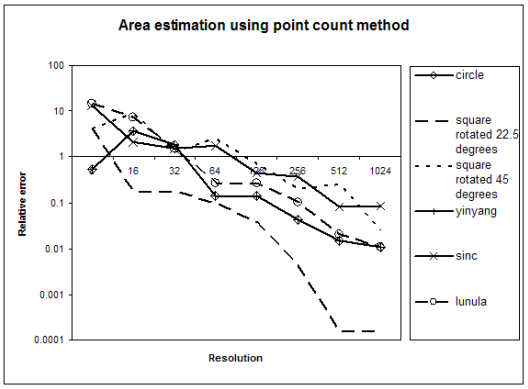

Fig. 10. Area estimation for the six test objects using the point count method with regular (grid-point) point probes.

Trends for circle and yinyang are similar due to the yinyang shape being formed by circular curves. The estimation for the square rotated 22.5° converges fastest, with an error of a bit more than 0.0001 percent at resolution 1024.

We also estimated volumes of 3D objects using the voxel count method with regular (grid-point) point probes, which is equivalent to applying the Cavalieri principle for a very special case (see discussion above).

The results in Figure 11 indicate reasonably small errors, which are all below 0.1 percent at picture resolution 1024. They all reflect multigrid and multiprobe convergent behavior (both are theoretically known) of the voxel count estimator on ellipsoid, cylinder, sphere and cube.

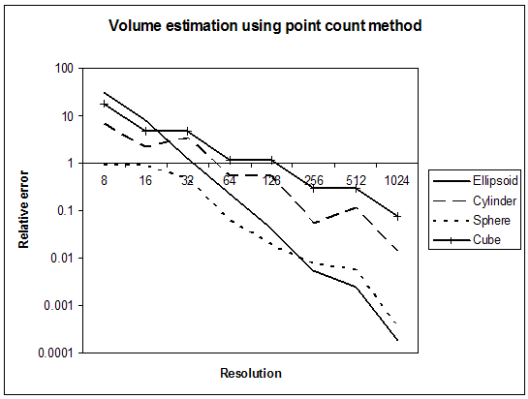

Fig. 11. Volume estimation for sphere, cube, ellipsoid, and cylinder using the Cavalieri principle in a special form (probes at all grid points in the 3D picture).

5 Conclusions

The point count estimators in stereology and digital geometry are different by motivation. Because a point is zero-dimensional, estimations using randomly chosen 2D or 3D points, or all pixels or voxels of the picture are unbiased and precise. Because estimators which use all pixel or voxel centers are very precise, there is no need to apply a random point generator for area and volume estimations.

If using the LICM for estimating perimeter or surface area, the IUR object-probe interaction must be guaranteed in order to make an unbiased observation of the object structure. Position or direction of the line probe cannot be pre-selected in this case to avoid bias. However, in our experiments a bias could not be totally removed even if lines of random directions are used (using a uniform number generator). It might be worth to spend more efforts on building an IUR line generator for the unbiased estimation of perimeter or surface area. Without such an ideal IUR line generator, the DSS-estimator appears to be the more time-efficient and faster converging method for perimeter estimations instead of the stereology estimator LICM.

The pixel and voxel count estimators for 2D area and volume are theoretically known to be multiprobe or multigrid convergent. Results for the DSS-estimator for length also corresponded to its known multigrid convergence, whereas the multiprobe convergence of the LICM estimator for length depends on the chosen line probes.

In practice, when the segmented objects are "complicated and irregular by shape", such as biological tissues and material microstructure, the stereology estimator LICM may be more efficient than the digital geometry estimator DSS as we do not need to trace all borders in the picture. In future experiments, more shapes generated randomly in size and position should be used and the average over all results of shapes should be considered.

Acknowledgement: The authors thank the reviewers of IWCIA for their valuable comments.

References

1. A.J. Baddeley, H.J.G. Gundersen, and L.M. Cruz-Orive. Estimation of surface area from vertical sections. *Journal of Microscopy*, **142**: 259-276, 1986.
2. J.E. Bresenham. Algorithm for computer control of a digital plotter. *IBM Systems Journal*, **4(1)**: 25-30, 1965.
3. B. Cavalieri. *Geometria Indivisibilibus Continuorum*. Typis Clementis Ferronij. Bononi. Reprinted (1966) as *Geometria degli Indivisibili*. Unione Tipografico-Editrice Torinese, Torino.
4. D. Coeurjolly and R. Klette. *A comparative evaluation of length estimators*. In *Proc. ICPR*, **IV**: 330–334, 2002.
5. I. Debled-Rennesson and J. Reveillès. A linear algorithm for segmentation of digital curves. *Int. J. Pattern Recognition and Artificial Intelligence*, **9**: 635-662, 1995.

6. J.D. Foley, A.V. Dam, S.K. Feiner, and J.F. Hughes. *Computer Graphics: Principles and Practice*, 2nd edition. Addison-Wesley, USA, 1996.
7. C.V. Howard and M.G. Reed. *Unbiased Stereology: Three-Dimensional Measurement in Microscopy*. BIOS Scientific Publishers, Oxford, 1998.
8. R. Klette, V. Kovalevsky, and B. Yip. On the length estimation of digital curves. Vision Geometry VIII, in *Proc. of SPIE*: 117-128, July 1999.
9. R. Klette and B. Yip. The length of digital curves. *Machine Graphics & Vision*,**9**: 673-703, 2000.
10. R. Klette and A. Rosenfeld. *Digital Geometry: Geometric Methods for Digital Picture Analysis*. Morgan Kaufmann, San Francisco, 2004.
11. V.A. Kovalevsky. New definition and fast recognition of digital straight segments and arcs. In *Proc. 10th Intl. Conf. on Pattern Recognition*, pages 31-34, 1990.
12. J. Lindblad. Surface area estimation of digitized planes using weighted local configurations. *DGCI 2003*, LNCS,**2886**: 348-357, 2003.
13. P.R. Mouton. *Principles and Practices of Unbiased Stereology: An Introduction for Bioscientists*. The Johns Hopkins University Press, Baltimore, 2002.
14. J. Ohser and F. Mücklich. *Statistical Analysis of Microstructures in Materials Science*. John Wiley, Chichester, 2000.
15. J.C. Russ and R.T. Dehoff. *Practical Stereology*, 2nd edition. Plenum, New York, 2000.
16. N. Sladoje, I. Nyström and P.K. Saha. Measuring perimeter and area in low resolution images using a fuzzy approach. *SCIA 2003*, LNCS, **2749**: 853-860, 2003.
17. E.E. Underwood. *Quantitative Stereology*. Addison Wesley, Reading MA, 1970.